

Toward modulating the architecture of hydrogel scaffolds: curtains versus channels

S. Van Vlierberghe · P. Dubruel · E. Lippens · B. Masschaele ·
L. Van Hoorebeke · M. Cornelissen · R. Unger · C. J. Kirkpatrick ·
E. Schacht

Received: 6 September 2007 / Accepted: 4 January 2008 / Published online: 26 February 2008
© Springer Science+Business Media, LLC 2008

Abstract The design, development and evaluation of biomaterials that can sustain life or restore a certain body function, is a very important and rapidly expanding field in materials science. A key issue in the development of biomaterials is the design of a material that mimics the natural environment of cells. In the present work, we have therefore developed hydrogel materials that contain both a protein (gelatin) and a glycosaminoglycan (chondroitin sulphate) component. To enable a permanent crosslinking, gelatin and chondroitin sulphate were first chemically modified using methacrylic anhydride. Hydrogels containing modified gelatin (gel-MOD) and/or chondroitin sulphate (CS-MOD) were cryogenically treated as optimised earlier for gel-MOD based hydrogels (Van Vlierberghe et al., *Biomacromolecules* 8:331–337, 2007). The cryogenic treatment leads to tubular pores for gel-MOD based systems. For CS-MOD based hydrogels and hydrogels containing both gel-MOD and CS-MOD, a curtain-like architecture (i.e. parallel plates) was observed,

depending on the applied CS-MOD concentration. In our opinion, this is the first paper in which such well-defined scaffold architectures have been obtained without using rapid prototyping techniques.

1 Introduction

The design, the development and the evaluation of biomaterials that can sustain life or restore a certain body function are very important and rapidly expanding topics in the field of material science. During the last few decades, regenerative medicine and tissue engineering have gained extensive attention. A frequently applied approach is the stimulation of the body ‘to heal itself’. Therefore, materials need to be developed which can function as cell carriers in vitro or which can be implanted in vivo with the aim to induce cell migration, adhesion and proliferation. In order to fulfil these requirements, the materials developed should meet some criteria. First, highly porous materials are required to support diffusion of oxygen and nutrients towards the cells and drainage of waste products from the matrix. Second, pore interconnectivity is crucial to enable cell migration and if required angiogenesis. Finally, the interconnecting porous biomaterials should be biocompatible and, depending on the application, also biodegradable [1, 2].

In the present work, porous hydrogel scaffolds based on gelatin and/or chondroitin sulphate will be evaluated as biomimetic materials. Gelatin is a biopolymer derived from collagen by hydrolytic degradation [3]. Due to its unique functionality, gelatin is used in a wide variety of applications, ranging from food-related [4, 5], over pharmaceutical [6] and photographic to technical products [7]. However,

S. Van Vlierberghe · P. Dubruel · E. Schacht (✉)
Polymer Chemistry & Biomaterials Research Group,
Ghent University, Krijgslaan 281 S4-bis, 9000 Ghent, Belgium
e-mail: Etienne.Schacht@UGent.be

E. Lippens · M. Cornelissen
Department of Human Anatomy, Embryology, Histology
and Medical Physics, Ghent University, Louis Pasteurlaan 2,
9000 Ghent, Belgium

B. Masschaele · L. Van Hoorebeke
Department of Subatomic and Radiation Physics,
Ghent University, Proeftuinstraat 86, 9000 Ghent, Belgium

R. Unger · C. J. Kirkpatrick
Institute of Pathology, Johannes Gutenberg University,
Langenbeckstrasse 1, 55101 Mainz, Germany

gelatin has also been frequently applied as a material for biomedical applications [8–10]. Chondroitin sulphate (CS) is a glycosaminoglycan composed of alternating units of *N*-acetyl-D-galactosamine and D-glucuronic acid [11]. Since it is a major component of the extracellular matrix, it has been applied before for tissue engineering purposes. Crosslinked gelatin-chondroitin sulphate-hyaluronan scaffolds were applied as biomimetic material for natural cartilage [12, 13]. The presence of chondroitin sulphate promoted the secretion of both proteoglycans and type II collagen [13]. Materials consisting of a gelatin-chondroitin sulphate-hyaluronan matrix have also been studied for wound treatment [14]. In addition to a histologically normal and adequately differentiated epithelial tissue, a well-defined dermal–epidermal junction and a collagen network were present in the dermis. The skin substitute had a positive effect on the promotion of the wound healing process and could be used to assist the regeneration of full-thickness skin defects [15, 16]. Another application of this scaffold was the regeneration of the human nucleus pulposus [17].

In a previous study of our research group, a method was described to produce chemically crosslinked porous gelatin hydrogels with a controlled pore size and pore morphology [18]. Chemically crosslinked gelatin hydrogels were treated cryogenically, with or without an applied temperature gradient between top and bottom of the scaffold. The matrices were then freeze-dried to remove the ice crystals formed. This resulted in porous hydrogels with specific and controlled pore size and morphology (channels versus spheres), depending on the applied cooling rate, gelatin concentration and temperature gradient [18]. The scaffolds developed were shown to be biocompatible, biodegradable and highly porous, favouring cell ingrowth [8].

In the present work, the development of hydrogels composed of gelatin and/or chondroitin sulphate are studied. The materials are compared in terms of their (physico)chemical properties using micro-computed tomography (μ -CT), optical microscopy, X-ray photo-electron spectroscopy (XPS), swelling experiments and atomic force microscopy (AFM). Preliminary in vitro biocompatibility studies are performed using confocal microscopy.

2 Materials and methods

2.1 Synthesis and characterization of hydrogel precursors

Chondroitin sulphate (1 g, 2 mmol disaccharide repeating units, 6 mmol hydroxyl functions, type C, Sigma–Aldrich) was dissolved in 50 ml double distilled water at room temperature. Subsequently, an excess methacrylic

anhydride (8.94 ml, 60 mmol, Sigma–Aldrich) was added dropwise. Simultaneously, the pH of the reaction mixture was adjusted to 8, by adding NaOH (5N). The methacrylic acid/NaOH ratio was 1. The mixture was then stirred at room temperature for 2 h. Finally, the solution was diluted with 50 ml double distilled water and transferred to a dialysis membrane (Spectra/Por® 3, Polylab, MWCO 3,500 Da, 3 days), followed by lyophilization.

The ^1H NMR spectrum of modified chondroitin sulphate (CS-MOD) was recorded at room temperature in deuterated water using a Bruker WH 500 MHz. The degree of substitution was calculated comparing the integrations (I) of the characteristic peaks of the methacrylate-substituent ($I_{1.95 \text{ ppm}}$, $I_{5.76 \text{ ppm}}$ and $I_{6.19 \text{ ppm}}$) and the methyl group from the CS *N*-acetyl group ($I_{2.04 \text{ ppm}}$) using the following equation:

$$\text{DS}(\%) = 3 \times 100 \times I_{5.76 \text{ ppm}} / (I_{1.95 \text{ ppm}} + I_{2.04 \text{ ppm}} - 3 \times I_{5.76 \text{ ppm}}) \quad (1)$$

The gelatin applied was isolated from bovine skin by an alkaline process (Rousselot). The material had an approximate iso-electric point of 5 and a Bloom strength of 257. The synthesis of methacrylamide modified gelatin (gel-MOD) was performed as described earlier [19]. Part of the amine functions of gelatin were reacted with methacrylic anhydride. For this work, a derivative with a degree of substitution of 60%, based on the lysine and hydroxylysine units, was used [19].

2.2 Hydrogel development

Using the gel-MOD and CS-MOD hydrogel precursors, different types of hydrogels were developed (Table 1). As an example, the 10 w/v% gel-MOD hydrogels (further referred to as type I hydrogels) were obtained by dissolving 1 g gelatin type B, previously modified with methacrylamide side groups, in 10 ml double distilled water at 40°C containing 2 mol% photo-initiator Irgacure® 2959 (Ciba Specialty Chemicals N.V.), as calculated to the amount of methacrylamide side chains. The solution was then injected into the mould of a cryo-unit, after which the solution was

Table 1 Hydrogel compositions

Hydrogel type	Gel-MOD	CS-MOD
I	10 w/v%	–
II		
A	10 w/v%	1 w/v%
B	10 w/v%	2 w/v%
C	10 w/v%	3 w/v%
D	10 w/v%	5 w/v%
III	–	10 w/v%

allowed to gel for 1 h at room temperature. In a final step, the hydrogel was exposed to UV-light (276 nm, 10 mW/cm², Vilber Lourmat) for 2 h, followed by applying a cryogenic treatment (cooling range on top side: 21°C until –30°C, cooling rate: 0.15°C/min). In addition, a temperature gradient ($T_{\text{top}} - T_{\text{bottom}} = 30^\circ\text{C}$) between top and bottom of the scaffold was applied during the freezing step. After incubating the sample for 1 h at the final freezing temperature, the frozen hydrogel was transferred to a freeze-dryer to remove the ice crystals, resulting in a porous scaffold [18].

CS-MOD based scaffolds and hydrogels containing both gel-MOD and CS-MOD (further referred to as, respectively, types III and II scaffolds) were developed by applying the same procedure as for the gel-MOD hydrogels. For type II hydrogels, the amount of CS-MOD was varied between 1 and 5 w/v%, while keeping the gel-MOD concentration constant (10 w/v%).

2.3 Hydrogel characterization

2.3.1 Hydrogel visualization

The architecture of the freeze-dried scaffolds developed was characterized using μ -CT (Skyscan 1072) [18]. After reconstruction of the 2D cross-sections, 3D software μ CTanalysis and Octopus were applied to enable 3D reconstruction.

The visualisation of freeze-sections of types I and II hydrogels after incubation at 37°C was performed by optical microscopy using an AxioTech 100 Reflected Light Microscope (Carl Zeiss), with reflected-light brightfield for Köhler illumination.

2.3.2 Hydrogel chemical composition

The chemical composition of the different scaffold surfaces was determined using FISON S-PROBE, a dedicated XPS (X-ray photoelectron spectroscopy) instrument designed to give the ultimate in performance, while providing a high sample throughput. The fine focus Al-K α source with a quartz monochromator, developed by Fisons Instruments Surface Science ensures lower background and higher sensitivity than conventional twin anode sources. All measurements were performed in a vacuum of at least 10^{–9} Pa. Wide and narrow-scan spectra were acquired at pass energy of 158 and 56 eV, respectively. The binding energy was calibrated by the C 1s peak at 284.6 eV. The spot size used was 250 μm on 1 mm. Data analysis was performed using S-PROBE software. The measured spectrum was displayed as a plot of the number of electrons (electron counts) versus electron binding energy in a fixed, small energy interval. Peak area and peak height sensitivity

factors were used for the quantifications. All data are expressed as atomic %.

2.3.3 Hydration properties of hydrogels

Freeze-dried samples ($1 \times 1 \times 0.5 \text{ cm}^3$) were weighed and then immersed in 80 ml double distilled water at 37°C, in the presence of NaN₃ to prevent bacterial growth. At regular time points, the hydrogels were removed from the solution, dipped gently with paper to remove excess water and weighed again. The hydration properties, expressed as the %water uptake, were calculated using the following equation:

$$\% \text{water uptake} = [(W_t - W_0)/W_0] \times 100\% \quad (2)$$

W_0 = initial weight of the dry scaffold, W_t = weight of the hydrated hydrogel at time point t .

All data points are the mean \pm standard deviation of three separate measurements.

2.3.4 Atomic force microscopy analysis

Phase separation phenomena upon mixing gel-MOD and CS-MOD were studied by AFM. Glass slides (\varnothing 1 cm) were spincoated with aqueous solutions of 5 w/v% gel-MOD with or without 1 w/v% CS-MOD during 90 s at 6,000 rpm. Next, AFM-studies were performed on the spincoated glass slides with a Nanoscope IIIa Multimode (Digital Instruments, Santa Barbara, California, USA) applying the ‘tapping mode’ in air.

2.4 In vitro cell interaction studies

The in vitro cell interaction of type I scaffolds was evaluated by applying human foreskin fibroblasts, glial cells (U373-MG) and epithelial cells (HELA) on the hydrogels, as described earlier [8]. Cells seeded on the hydrogel were visualised within the hydrogels at different time points using confocal microscopy. Cell-seeded hydrogels were first incubated with calcein-AM (1 $\mu\text{g}/\text{ml}$) for 5–10 min at 37°C in the dark. Calcein-AM is a cell-permeable compound which is taken up by viable cells and subsequently hydrolysed by intra-cellular esterases. Upon hydrolysis, calcein-AM becomes highly fluorescent and cell-impermeable which makes it suited for vital cell visualisation purposes. After the incubation step, the hydrogels were transferred into a petri-dish for confocal microscopy analysis (Leica TCS NT) [8].

3 Results and discussion

In the present work, we have developed and compared different types of hydrogels based on gelatin and/or

chondroitin sulphate. By combining both protein and glycosaminoglycan molecules into one porous hydrogel material, we aimed to develop biomimetic hydrogel materials. The materials developed were compared in terms of their chemical composition, 3D structure and water uptake capacity. Preliminary in vitro biocompatibility studies were also performed.

3.1 Synthesis and characterization of hydrogel precursors

Two different types of biopolymers were selected for the production of hydrogel materials: gelatin and CS. Since gelatin possesses a sol–gel temperature below body temperature, a derivatisation reaction of both biopolymers was performed, enabling the production of permanently cross-linked hydrogel networks.

The introduction of crosslinkable methacrylamide groups onto gelatin by reaction of the primary amines from the lysine and hydroxylysine units was reported before [18]. Using a similar protocol, part of the hydroxyl groups of CS were converted into methacrylate groups (see Fig. 1). As methacrylic acid (MA) is generated during the esterification, NaOH was added as neutralizing agent, avoiding possible acid catalysed degradation of the polysaccharide. The glycosaminoglycan containing crosslinkable methacrylate groups was purified by membrane dialysis against double distilled water for several days, followed by isolation via lyophilization. A typical ^1H NMR spectrum of a functionalised CS is shown in Fig. 2. The degree of substitution was calculated comparing the integrations of the characteristic vinyl (5.76 and 6.19 ppm for $\text{C}=\text{CH}_2$ and 1.95 ppm for $\text{CH}_3-\text{C}=\text{CH}_2$) and CS protons ($\text{CH}_3-\text{CO}-\text{NH}-$) using Eq. 1 (see Sect. 2.1).

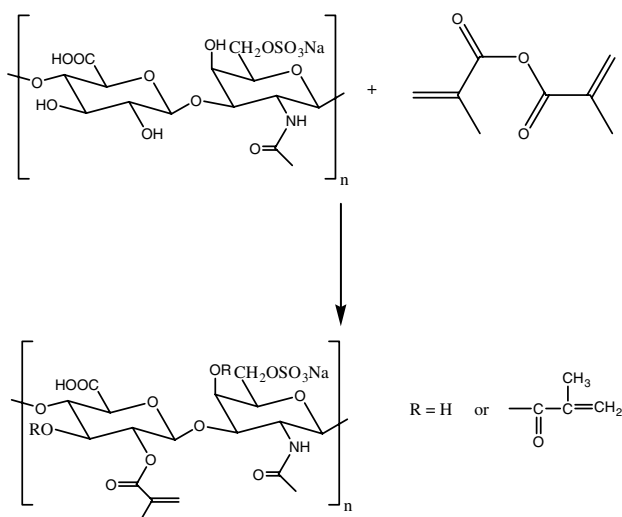


Fig. 1 Synthesis of chondroitin sulphate-methacrylate

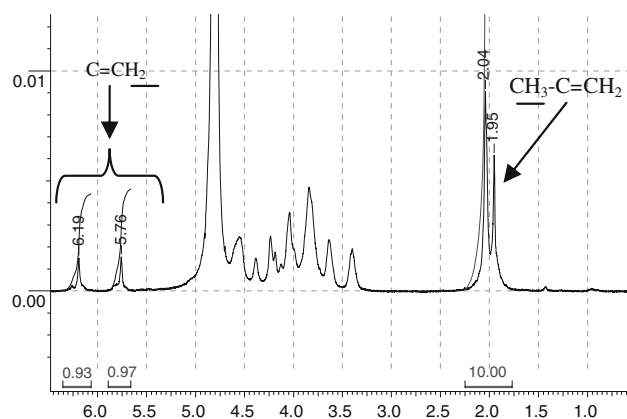


Fig. 2 ^1H NMR spectrum of chondroitin sulphate-methacrylate

The degree of substitution obtained was 40% relative to the amount of disaccharides (i.e. 40% of all disaccharide units contain one double bond). In the text below, the functionalised biopolymers will be indicated as gel-MOD and CS-MOD.

3.2 Production of porous hydrogels

Using the hydrogel precursors synthesised, a series of hydrogels was prepared by applying a cryogenic treatment on gel-MOD, CS-MOD or combinations of both gel-MOD and CS-MOD (Table 1). In what follows, hydrogels containing gel-MOD as biopolymer are indicated as type I hydrogels. Hydrogels containing both gel-MOD and CS-MOD are indicated as type II hydrogels. Hydrogels composed of CS-MOD only are indicated as type III hydrogels. Types I and II hydrogels contain 10 w/v% gel-MOD. For type II hydrogels, the amount of CS-MOD was varied between 1 and 5 w/v% (type II A–D). Type III hydrogels contain 10 w/v% CS-MOD.

All hydrogels were formed by gelation of (mixtures of) aqueous biopolymer solutions at room temperature, followed by radical UV-induced photo-crosslinking (photo-initiator: Irgacure 2959). Then, the chemically crosslinked hydrogels were subjected to a cryogenic treatment. The different materials developed are summarised in Table 1.

3.3 Hydrogel evaluation

3.3.1 Hydrogel visualisation

The scaffolds developed were characterized using μCT and optical microscopy to obtain information about the pore architecture and the pore size. Micro-CT measurements demonstrated that type I hydrogels contained top bottom transversal channels with a decreasing pore size from top to bottom (330–20 μm) (Fig. 3, left column). The applied temperature gradient resulted in hydrogel materials with a

pore size gradient. In contrast to what was anticipated, a similar cryogenic treatment applied to hydrogels containing only CS-MOD (type III hydrogels) lead to materials with deviating pore geometry: a curtain-like geometry consisting of 200 μm spaced parallel plates was observed, as indicated in Fig. 3 (right column). This is most likely due to the parallel stacking of the water-binding glycosaminoglycan chains, as depicted schematically in Fig. 4. Indications supporting this assumption were already described previously in literature [20, 21]. To the best of our knowledge, such well-defined scaffold architectures have so far only been obtained using rapid prototyping techniques [22]. The present work clearly shows that depending on the biopolymers applied, biomimetic materials with varying pore geometries can be easily developed. This unique curtain-like design offers potential for cell sheet engineering. If required, the ‘curtains’ can be coated in a separate step using cell-interactive peptides or proteins enabling specific cell–material interactions.

For hydrogels containing both gel-MOD and CS-MOD (type II hydrogels), a curtain-like architecture was also obtained. However, in contrast to type III hydrogels, no parallel plates were observed. It can be anticipated that the observed differences are due to the lower amount of CS-MOD in type II hydrogels compared to type III hydrogels.

In a subsequent part of the work, the scaffold structures were visualised after incubation in double distilled water at 37°C. In this way, we could investigate whether the

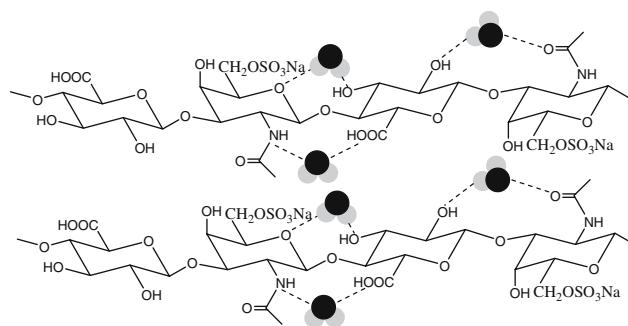
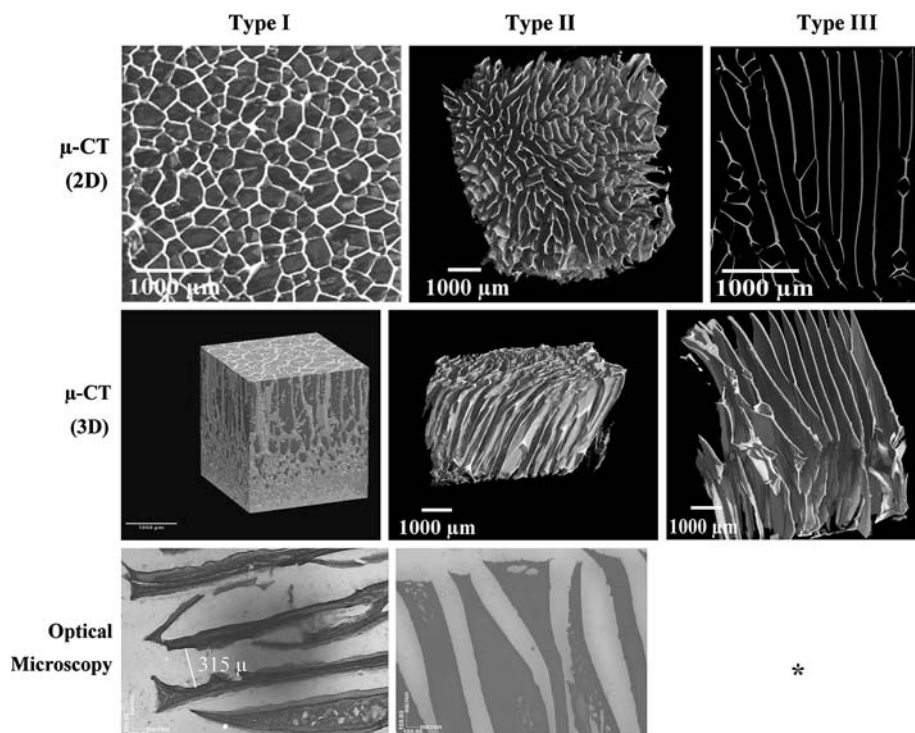


Fig. 4 Overview demonstrating possible interactions existing between CS and water molecules

scaffold architectures are preserved after *in vivo* or *in vitro* application. Unfortunately, μCT imaging on swollen hydrogels leads to blurred images due to the full hydration of the polymer chains at equilibrium swelling. This can be ascribed to differences in density or atomic number which are too small to enable visualisation by μCT. To solve this problem, freeze-sections of the swollen matrices were stained and visualized by optical microscopy (Fig. 3, bottom part). Types I and II hydrogels were sectioned, respectively, longitudinal and transversal. From the freeze-section images, it can be concluded that the scaffold architectures (i.e. elongated channels for type I hydrogels and curtain-like for type II scaffolds) were preserved after incubating the hydrogels at body temperature. Moreover, no significant changes in pore size were observed upon

Fig. 3 μCT (2D and 3D) and optical microscopy analysis of gel-MOD (type I), CS-MOD (type III) and a hydrogel containing gel-MOD and CS-MOD (type II). The scale bars represent 1,000 μm (μ-CT) and 100 μm (optical microscopy). * = No data available (hydrogel burst during swelling)



comparing the freeze-dried scaffolds with the freeze-section images of swollen hydrogels. Type III hydrogels were not freeze-sectioned because of their very high swelling potential, often resulting in scaffold cracking. The latter is due to the presence of sulphate groups in CS-MOD, which are able to retain large amounts of water. Types I and II hydrogels contain gelatin, which is a physical structuring polymer, which is absent in type III materials [23].

3.3.2 Hydrogel chemical composition

The observed differences in pore geometry between types I and II hydrogels were a first indication that both gel-MOD and CS-MOD were introduced in type II hydrogel networks. To further confirm these findings, a series of XPS measurements were performed (see Table 2). The sulphur signal appearing in all type II hydrogels confirms the presence of CS in the developed materials. This characteristic signal was not observed for type I hydrogels containing only gel-MOD. Type I hydrogels exhibited higher nitrogen (10%) and no sulphur compared with type III hydrogels (3% and 4%, respectively). This can be ascribed to the fact that the amount of sulphur-containing amino acids in gel-MOD is too low (0.4% of all amino acids are methionine) to be detected by XPS, which makes it a useful technique for indicating the presence of CS in the newly developed hydrogels. Furthermore, incubation at 37°C for 24 h revealed no significant changes in chemical composition, further indicating a successful covalent immobilisation of the CS-MOD in the type II hydrogel networks.

3.3.3 Water uptake capacity

For a tissue engineering scaffold, it is important to absorb body fluids and transfer nutrients and metabolites to/from implanted cells [24]. Therefore, we studied the water uptake capacity of type II hydrogels by incubation in double distilled water at 37°C, while monitoring the water uptake at regular time points. The results are summarised in Fig. 5. It can be concluded that the water uptake capacity at equilibrium swelling decreases with an increasing amount of CS-MOD in the hydrogels. Since

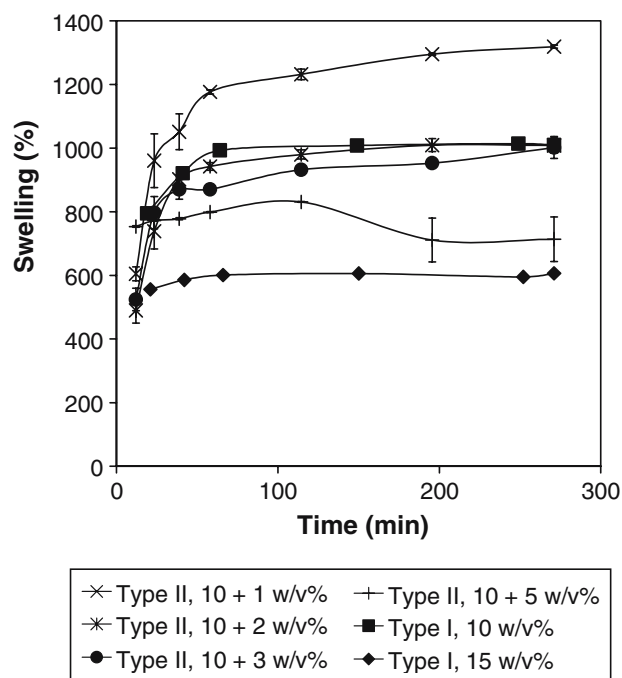


Fig. 5 Influence of the chondroitin sulphate concentration (1–5 w/v%) on the hydration properties of hydrogels composed of 10 w/v% gel-MOD and comparison with the water uptake capacity of 10 w/v% and 15 w/v% type I hydrogels. The values represent the average of three measurements ($n = 3$, SD)

CS-MOD contains a higher amount of functional groups that can be crosslinked compared to gel-MOD, a higher amount of CS-MOD in the hydrogels leads to materials with a higher crosslink density and thus a lower water uptake capacity.

In order to evaluate the effect of the CS incorporation in type II hydrogels, while excluding the influence of the polymer concentration, the water uptake of 15 w/v% type I hydrogels (containing only gel-MOD) were compared with type II hydrogels consisting of 5 w/v% CS-MOD (D) and 10 w/v% gel-MOD. From Fig. 5, it can be concluded that the incorporation of chondroitin sulphate into pure gelatin-based scaffolds results in an increase of the water uptake capacity, due to the presence of the CS sulphate groups. This was further confirmed by comparing the equilibrium swelling degree of a scaffold, composed of 10 w/v% gel-MOD and 1 w/v% CS-MOD (type II, A), with an identically cryo-treated 10 w/v% gel-MOD hydrogel (type I) (i.e. 1,300% vs. 1,000%) [25].

3.3.4 Atomic force microscopy analysis

Since scaffold staining using various dyes (Alcian blue, Rhodamine B, dextran blue, Ninhydrin) did not enable a selective visualization of neither gelatin nor chondroitin sulphate, AFM was applied to study possible phase

Table 2 Elemental composition of the samples determined by XPS

Sample	Atomic composition (%)			
	C	N	O	S
Type I	72 ± 3	10 ± 3	18 ± 1	–
Type II	60 ± 3	9 ± 1	30 ± 3	1 ± 1
Type II (inc.)	60 ± 1	11 ± 1	25 ± 1	1 ± 1
Type III	57 ± 3	3 ± 1	35 ± 5	4 ± 1

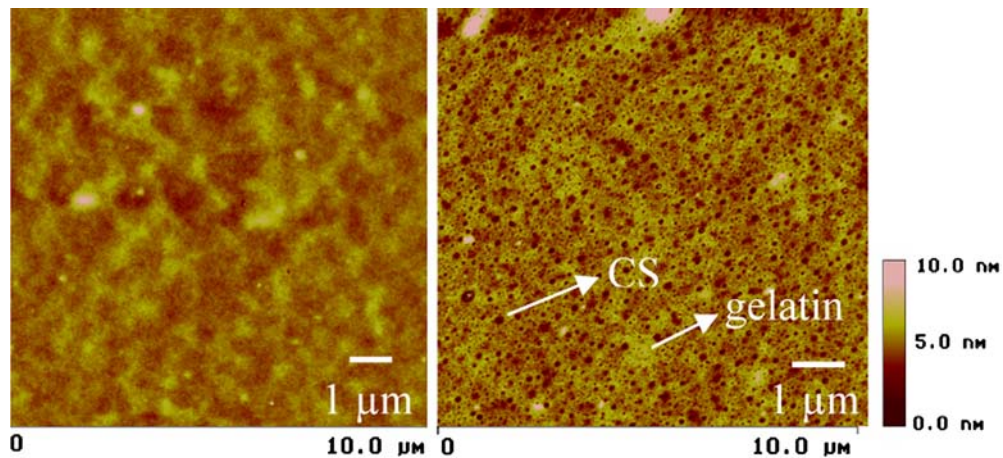


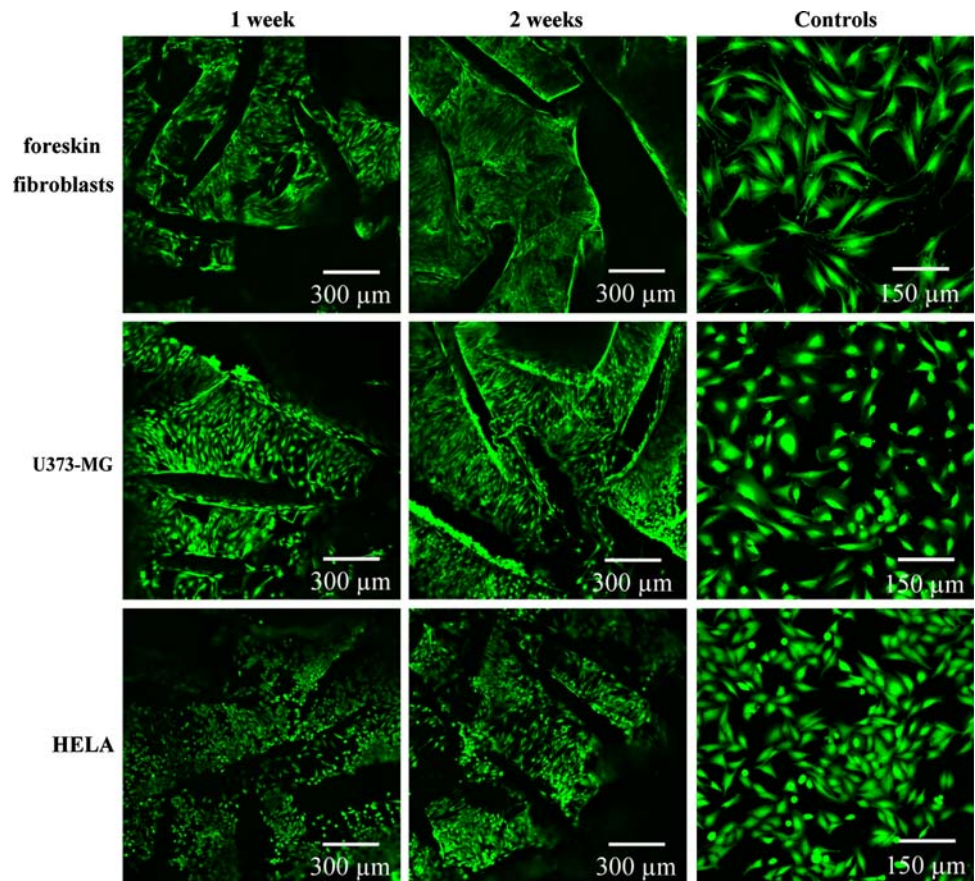
Fig. 6 Height images of gel-MOD (left) and gel-MOD + CS-MOD scaffolds (right), obtained using AFM. The scale bars represent 1 μm and 10 nm

separation phenomena between both biopolymers. This might explain the mechanisms leading to the curtain-like pore architecture for type II hydrogels.

The measurements were performed on spincoated gel-MOD/CS-MOD solutions since preliminary AFM measurements indicated the requirement of flat surfaces. In addition to the globular domains of gel-MOD (Fig. 6, left

part), mixtures of gel-MOD and CS-MOD contain smaller regions of phase-separated CS-MOD (Fig. 6, right part). We anticipate that both phase separation between gel-MOD and CS-MOD and the parallel stacking of the water-binding CS-MOD chains are responsible for the curtain-like scaffold architecture obtained by combining both biopolymers. At present, we are further studying these

Fig. 7 Human foreskin fibroblasts, U373-MG and HELA visualisation (10× magnification) on type I hydrogels at different time points after cell seeding (left part). Visualisation (20× magnification) of tissue culture plastic (TCP) seeded foreskin fibroblasts, U373-MG and HELA (right part). Cells were stained with calcein-AM (1 μg/ml) and visualised using confocal microscopy. The scale bars represent 150 and 300 μm



phenomena in detail to identify the mechanisms underlying these findings.

3.3.5 Preliminary *in vitro* biocompatibility studies

In a final part of this work, type I hydrogels were screened for their *in vitro* biocompatibility properties. The adhesion, spreading and proliferation of human foreskin fibroblasts, glial cells (U373-MG) and epithelial cells (HELA) was studied by confocal microscopy analysis of calcein-AM labelled cells. For the preliminary experiments performed, cell visualisation was performed on the same side of the scaffold on which the cells were seeded. The results after 1 and 2 weeks incubation (Fig. 7) clearly indicate that all cell types adhere, spread and proliferate after cell seeding. At present, we are evaluating the potential influence of the curtain-like architecture (i.e. types II and III hydrogels) on the cellular behaviour. The results will be the topic of a forthcoming paper.

4 Conclusions

In the present work, highly porous biomimetic hydrogels based on a combination of gelatin and chondroitin sulphate (CS) have been studied. After the functionalisation of both biopolymers with crosslinkable groups, gelatin hydrogels, CS hydrogels and hydrogels containing both gelatin and CS were prepared and cryogenically treated. It was shown that variation of the hydrogel composition (i.e. increasing the amount of CS), leads to a modulation of the scaffold architecture. For gelatin based hydrogels, a channel-like pore morphology was obtained. CS-based hydrogels and hydrogels containing both gelatin and CS possessed a curtain-like pore architecture. To the best of our knowledge, materials with such well defined pore geometries have not yet been reported. The materials composed of parallel plates offer a potential for a variety of applications, e.g., as cell carriers. Moreover, the material can be coated with cell-interactive peptide sequences to stimulate selective cell interactions.

The influence of the scaffold architecture (i.e. channel versus curtain) on the cellular behaviour is currently being evaluated. The results will be reported in a forthcoming paper.

Acknowledgements The authors would like to acknowledge the Institute for the Promotion of Innovation by Science and Technology

in Flanders (IWT) for the Ph.D. funding granted to S. Van Vlierberghe, the Alexander von Humboldt Foundation for the financial support under the form of a granted Research Fellowship and the Belgian Research Policy Inter University Attraction Poles (IUAP/PAI-V/03) for financial support.

References

1. H.W. Kang, Y. Tabata, Y. Ikada, *Biomaterials* **20**, 1339 (1999)
2. F.J. O'Brien, B.A. Harley, I.V. Yannas, L. Gibson, *Biomaterials* **25**, 1077 (2004)
3. S.M. Tosh, A.G. Marangoni, F.R. Hallett, I.J. Britt, *Food Hydrocolloids* **17**, 503 (2003)
4. J. Adler-Nissen, in *Enzymic hydrolysis of food proteins* (Elsevier Applied Science Publishers Ltd., London and New York, 1985)
5. A.G. Ward, A. Courts, in *The science and technology of gelatin* (Academic Press, London, New York and San Francisco, 1977)
6. R. Narayani, K.P. Rao, *Int. J. Pharm.* **128**, 261 (1996)
7. K.B. Djagny, Z. Wang, S.Y. Xu, *Crit. Rev. Food Sci. Nutr.* **41**, 481 (2001)
8. P. Dubruel, R. Unger, S. Vanvlierberghe, V. Cnudde, P.J.S. Jacobs, E. Schacht, C.J. Kirkpatrick, *Biomacromolecules* **8**, 338 (2007)
9. A.K. Bajpai, J. Choubey, *J. Macromol. Sci.-Pure Appl. Chem.* **A42**, 253 (2005)
10. A.J. Kuijpers, P.B. Van Wachem, M.J.A. Van Luyn, L.A. Brouwer, G.H.M. Engbers, J. Krijgsveld, S.A.J. Zaat, J. Dankert, J. Feijin, *Biomaterials* **21**, 1763 (2000)
11. R.L. Jackson, S.J. Busch, A.D. Cardin, *Physiol. Rev.* **71**, 481 (1991)
12. C.H. Chang, T.F. Kuo, C.C. Lin, C.H. Chou, K.H. Chen, F.H. Lin, H.C. Liu, *Biomaterials* **27**, 1876 (2006)
13. C.H. Chang, H.C. Liu, C.C. Lin, C.H. Chou, F.H. Lin, *Biomaterials* **24**, 4853 (2003)
14. T.-W. Wang, J.-S. Sun, H.-C. Wu, Y.-H. Tsuang, W.-H. Wang, F.-H. Lin, *Biomaterials* **27**, 5689 (2006)
15. T.W. Wang, H.C. Wu, Y.C. Huang, J.S. Sun, F.H. Lin, *Artif. Organs* **30**, 141 (2006)
16. T.W. Wang, J.S. Sun, H.C. Wu, Y.H. Tsuang, W.H. Wang, F.H. Lin, *Biomaterials* **27**, 5689 (2006)
17. S.H. Yang, P.Q. Chen, Y.F. Chen, F.H. Lin, *Artif. Organs* **29**, 806 (2005)
18. S. Vanvlierberghe, V. Cnudde, P. Dubruel, B. Masschaele, A. Cosijns, I. Depaepe, P.J.S. Jacobs, L. Vanhoorebeke, J.P. Remon, E. Schacht, *Biomacromolecules* **8**, 331 (2007)
19. A.I. Van Den Bulcke, B. Bogdanov, N. De Rooze, E.H. Schacht, M. Cornelissen, H. Berghmans, *Biomacromolecules* **1**, 31 (2000)
20. A. Almond, *Carbohydr. Res.* **340**, 907 (2005)
21. J. Seog, D. Dean, B. Rolauffs, T. Wu, J. Genzer, A.H.K. Plaas, A.J. Grodzinsky, C. Ortiz, *J. Biomech.* **38**, 1789 (2005)
22. R. Landers, U. Hubner, R. Schmelzeisen, R. Mulhaupt, *Biomaterials* **23**, 4437 (2002)
23. M. Djabourov, *Contemp. Phys.* **29**, 273 (1988)
24. L. Peng, X.R. Cheng, J.W. Wang, D.X. Xu, G. Wang, *J. Bioact. Compat. Polym.* **21**, 207 (2006)
25. S. Vanvlierberghe, P. Dubruel, E. Lippens, M. Cornelissen, E. Schacht, *J Biomater Sci Polym Ed*, Submitted (2008)